

FFF 3D Printing of Small Porous Structures from Polymer Compounds Using the Ultimaker 3

Matthias F. Ernst, Annabelle Maletzko, Sascha Baumann, Nils Baumann, Christof Hübner, and Carl-Christoph Höhne*

Additive manufacturing offers a great potential for the production of objects with a tailor-made inner structure especially in combination with material development in the field of polymer compounds. However, the design possibilities for the inner structure depend on printing resolution, accuracy, and reproducibility. The quality of small filigree objects printed by additive manufacturing processes for polymer materials like fused filament fabrication (FFF) depends on the polymer material itself as well as on the processing parameters in the additive manufacturing technology used. Here, the production of small porous structures by FFF with an Ultimaker 3 is analyzed using polylactic acid (PLA) as well as polymer compounds of PLA containing carbon nanotubes (CNTs) and polyvinyl alcohol (PVA) containing titanium dioxide (TiO₂). The influences of the calibration of the building plate, the heights of the 1st, 2nd, and 3rd layers, and of particulate additives on the printing behavior of the polymer compound, and hence the resulting accuracy of the width of single printed lines, are studied. Additionally, the printing of lattice-like scaffold structures using PLA/CNT forming the structure and PVA/TiO₂ as soluble support structure is described.

object. However, a tailor-made inner structure is particularly interesting for many applications especially when the inner structure interacts with the environment such as within a porous catalyst layer, within absorber materials, within a flow field for fluids, or other applications. The inner structure is also highly important for the mechanical stability and mechanical behavior of the object, for example, for lightweight components with local reinforcements. Additive manufacturing (AM) – “3D printing” – enables a systematic layer-by-layer buildup of an object as 3D objects are created by stacking individual layers on top of each other. The possibility to adapt the structure of each layer individually offers a great potential, especially for creating tailor-made inner structures down to microscale in comparison to other shaping processes. However, to allow as much freedom as possible in the design of the inner structure, the smallest possible structures must be reproducible and accurately producible by AM. In

1. Introduction

Giving an object a complex outer shape is simple compared to the effort required to specifically shape the inner structure of an

this paper, the AM technique fused filament fabrication (FFF) of plastic compounds is discussed.

Filigree porous structures manufactured by FFF have been investigated, especially in the context of biomedical applications. In most of these studies, mesh-like structures of several layers were manufactured with road widths ranging from 0.18 mm to 0.98 mm and layer heights from 0.15 mm to 0.4 mm, leading to porosities in the large range of 8–70%.^[1,2] In several investigations, composite materials have been used to create tissue engineering scaffolds by FFF. The polymer additives of these composites include hydroxyapatite,^[3] tricalcium phosphate,^[4] bioactive glass,^[2] or graphene oxide.^[5] Similar mesh-shaped porous objects might also be useful for other applications as the pore size and porosity can be customized, and such objects feature uniform pore sizes or defined size variations in contrast to other porous media like foams or felts.

The quality of these filigree porous structures produced by AM thereby depends on the AM technology used. For common structural applications, the quality of an object produced by AM processes is usually described by dimensional accuracy, resolution, surface roughness, and mechanical properties. These mentioned quality characteristics are affected by several main factors as product design parameters, process parameters, system limitations/errors, technical characteristics of the AM device, and

M. F. Ernst
Chair of Technical Electrochemistry
Technical University of Munich
Lichtenbergstraße 4, 85748 Garching, Germany
A. Maletzko, S. Baumann, C. Hübner, C.-C. Höhne
Fraunhofer Institute for Chemical Technology ICT
Joseph-von-Fraunhofer-Straße 7, D-76327 Pfinztal, Germany
E-mail: carl-christoph.hoehne@ict.fraunhofer.de
N. Baumann
Proton Motor Fuel Cell GmbH
Benzstraße 7, 82178 Puchheim, Germany

 The ORCID identification number(s) for the author(s) of this article can be found under <https://doi.org/10.1002/mame.202200095>

© 2022 The Authors. Macromolecular Materials and Engineering published by Wiley-VCH GmbH. This is an open access article under the terms of the Creative Commons Attribution-NonCommercial-NoDerivs License, which permits use and distribution in any medium, provided the original work is properly cited, the use is non-commercial and no modifications or adaptations are made.

DOI: 10.1002/mame.202200095

properties of the polymeric material. According to Turner and Gold,^[6] dimensional accuracy, resolution, and surface roughness are functions of process and product design parameters. The manufacturing of small porous structures like lattice-like structures of, for example, 500 μm height by FFF is affected by most of the abovementioned parameters. In contrast to common 3D-printing applications, the most determining quality characteristics of small porous structures are dimensional accuracy and resolution, in particular the minimal achievable resolution in layer height and line width as well as dimensional accuracy in layer height and line width. The main influences on the dimensional accuracy and resolution are assumed to be the technical characteristics of the AM device as well as the properties of the polymeric material.

In this paper, an Ultimaker 3 FFF desktop 3D printer with two printheads is used. This type of FFF printer uses an extrusion-based AM process where the desired product is built-up in layers from a thermoplastic 2.85 mm filament. For each printhead, a feeder pushes the filament through a Bowden tube into the printhead where it melts and is then extruded through a nozzle onto a heated glass build plate or the previously printed layer, respectively. At the same time, the printhead unit moves horizontally at a distinct height over the print bed which leads the extrudate to form a line. When printing a line directly next to an existing one, they merge to form a 2D structure. By moving down the build plate, several 2D layers can be placed on top of each other to create a "3D-printed" object.^[7] Ultimaker indicates an accuracy of 12.5 μm for x and y positioning and 2.5 μm for z positioning.^[8]

Objects featuring large overhangs require support structures to be built by this layer-by-layer approach. In FFF, these supporting scaffold structures are commonly built from soluble material, e.g., water-soluble polymers like polyvinyl alcohol (PVA) offering removal in postprocessing.^[9]

FFF printers can be equipped with multiple printheads allowing to create multimaterial objects.^[10] The Ultimaker 3 contains two printheads which can be equipped with different types of nozzles, e.g., 0.25 mm nozzle with a layer resolution of 150–60 μm , 0.40 mm nozzle with a layer resolution of 200–20 μm , and 0.80 mm nozzle with a layer resolution of 600–20 μm ^[8] as well as nozzles with a different inner shape in the area of the radius narrowing as type-AA nozzle which is staged at the nozzle outlet to reduce oozing of material and type-BB nozzle with a smooth radius narrowing to prevent clogging of material.

The technical properties of an AM device are to a wide extent not accessible to the user, except the planarity of the building plate, the calibration of the building plate position, the nozzle type, and the nozzle diameter.

The polymeric composite material of the printing filament also shows a main influence on the dimensional accuracy and resolution. Beside the thermoplastic properties needed for the FFF process, the composite shows specific material properties needed to achieve tailored object functionalities, for example, electrical conductivity. Depending on the desired properties, composites used in FFF contain different additives, for example, pigments for coloring, fibers for improved mechanical strength,^[11] metal particles for higher hardness,^[12] carbon nanotubes for improved electrical conductivity,^[13] or active pharmaceutical ingredients to be released from FFF-printed medical devices.^[14] The use of 2.85 mm filaments in the Ultimaker 3 can be advantageous com-

pared to 1.75 mm filaments of other FFF devices, especially for the 3D printing of compounds with high additive content.

The aim of the work is to study how small porous structures can be produced by FFF using an Ultimaker 3. Especially, the minimum printable layer height and line width are the focus of the investigations. For this purpose, the influence of the method for the calibration of the distance between building plate and printing nozzle and the minimum printable height of the first three layers of 3D printed small plates were studied using polylactic acid (PLA). Based on these results, compounds of PLA and carbon nanotubes (CNTs) as well as compounds of PVA and titanium dioxide (TiO_2) were investigated by analyses of the filament extrusion properties and of the minimum line width of single 3D printed lines. Finally, a small porous structure of PLA–CNT was produced.

2. Results and Discussion

The main influences on the dimensional accuracy and resolution are assumed to be the technical characteristics of the AM device as well as the properties of the polymeric material. To avoid inaccuracies of product design parameters and process parameters of the AM device, the G-codes, which contain the commanding process parameters and toolpath for the 3D printer, of the models printed for this paper were manually created and not by a slicing software.

The polymeric material influences the dimensional accuracy and resolution particularly by shrinkage due to crystallization processes. However, an influence on dimensional accuracy and resolution minor for the studied line height and line width by the used polymeric materials is assumed to be due to the used sample geometry.

2.1. Calibration of the Distance between Building Plate and Printing Nozzle

3D printing of small structures with only a few thin layers by FFF requires a precise calibration as the distance between build plate and printing nozzle significantly influences the printing results especially of the first layers. The Ultimaker 3 FFF printer possesses an active leveling routine (autocalibration) which measures the distance between the tip of the nozzle and the build plate at different locations. Inaccuracies of the build plate level are compensated during the printing of the first layer of the print by slightly adjusting the build plate height while printing.^[8] This method is unsuitable for printing a first layer with a defined thickness.

Furthermore, the horizontal orientation of the building plate can be adjusted manually by adjusting three screws located in two of the corners and in the middle of one edge of the building plate holder (manual leveling).^[8] This manual calibration routine can also be used to set the absolute distance between build plate and printing nozzle by placing a reference spacer between these two and tightening the adjusting screw until a noticeable friction occurs when moving the spacer horizontally.

To study the calibration influence on the first layer height, the distance between build plate and nozzle was adjusted using both



Figure 1. Generic step-like profile illustrating the nomenclature used in this work.

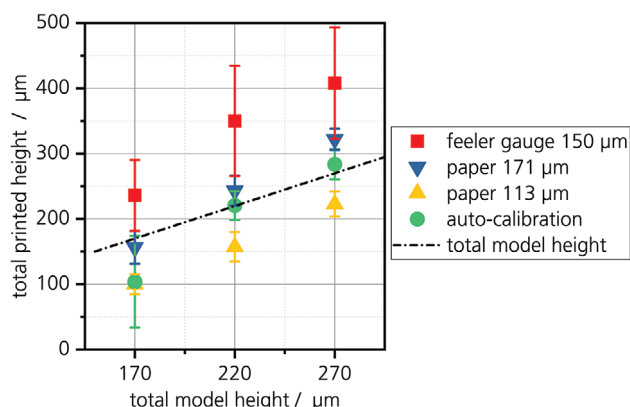


Figure 2. Total thickness of the first, second, and third steps of a test sample printed with PLA by using three different manual calibration methods and the autocalibration.

auto- and manual calibration. Three different types of spacers were employed for the latter routine: a) A4 printing paper with a thickness of $113 \pm 5 \mu\text{m}$, b) a paper with a thickness of $171 \pm 5 \mu\text{m}$, and c) a feeler gauge with a thickness of $150 \mu\text{m}$. For each spacer, a test sample of $20 \times 60 \text{ mm}^2$ and a step-like profile with a thickness of $170 \mu\text{m}$ for the first layer (first step) and a thickness of $50 \mu\text{m}$ for the second layer (second step) and third layer (third step) were printed using PLA. This leads to a nominal second and third total heights of $220 \mu\text{m}$ and $270 \mu\text{m}$, respectively.

Figure 1 illustrates the nomenclature of the step-like profiles used in this work. The results of the calibration experiments are shown in Figure 2.

As shown in Figure 2, the autocalibration routine leads to an intolerable variance of the first layer height. Therefore, it is not suitable for the printing of small single layer objects. Presumably, this is because the autocalibration routine compensates inaccuracies of the build plate level during the printing of the first layer. However, the total thicknesses of the second and third steps show the lowest deviation from the model thicknesses if the autocalibration is used. For single layer prints with $170 \mu\text{m}$ thickness, a calibration with paper of $171 \mu\text{m}$ thickness shows the best match with a 1^{st} layer height of $157 \mu\text{m}$. Calibration with the paper of $113 \mu\text{m}$ thickness as well as the autocalibration lead to significantly lower 1^{st} layer thicknesses of about $100 \mu\text{m}$. Similar observations are also reported in literature for the Ultimaker 3 FFF printer, e.g., $48 \mu\text{m}$ print height is observed for a model thickness of $63 \mu\text{m}$ printed with a $100 \mu\text{m}$ nozzle and $160 \mu\text{m}$ print height is measured for a model thickness $180 \mu\text{m}$ printed with a $400 \mu\text{m}$ nozzle.^[15] For the feeler gauge with $150 \mu\text{m}$ thickness, a significantly higher 1^{st} layer thickness of $236 \mu\text{m}$ is observed. This calibration routine leads to systematically larger variations of the object height compared to the other investigated options.

One possible reason for this might be the different interactions between the calibration spacer and the Ultimaker's metal printing nozzle. A metal-on-metal contact makes it more difficult for the experimenter to sense a certain frictional resistance in a reproducible way, compared to a metal on paper contact, where the metal tip of the nozzle can sink into the paper to a certain degree.

Besides the careful adjustment of the build plate, the quality of the building plate is essential, as an uneven build plate will result in an uneven printing layer thickness particularly in the first layer. The height of the build plates used in this work varies by maximum $15 \mu\text{m}$ (measured by a micrometer, accuracy of $\pm 1 \mu\text{m}$) along their entire length ($\geq 230 \text{ mm}$). For small objects (e.g., one step of $20 \times 30 \text{ mm}^2$), this surface variation of the build plate lies in the range of $1\text{--}3 \mu\text{m}$. Therefore, the influence of a possibly uneven build plate on the layer height (experimental standard deviation minimum $\pm 15 \mu\text{m}$) can be neglected.

To achieve reproducible printing qualities, a calibration of the building plate should be performed for each printing. Several structures can be produced in one print by placing them next to each other on the build plate. Ideally, the calibration distance between printing nozzle and build plate lies in the range of the desired printing layer height. For the printing of small single layer objects, the autocalibration routine is not suitable.

2.2. Minimum Height of the 1^{st} , 2^{nd} , and 3^{rd} Layers of 3D Printed Small Plates

The printing quality of the 1^{st} layer is highly important for the 3D printing of small structures as small structures typically consist only of a few layers whereby occurring deviations cannot be compensated. To study the influence of the layer height on the print quality of the first three layers, step-like models were printed with PLA using a type-AA nozzle with $250 \mu\text{m}$. According to Ultimaker,^[8] the minimum height of this type-AA nozzle is in the range of $60\text{--}150 \mu\text{m}$.

The first layer was printed with $50 \mu\text{m}$, $100 \mu\text{m}$, or $150 \mu\text{m}$. On top of each 1^{st} layer, two layers with $25 \mu\text{m}$ or $50 \mu\text{m}$ each were printed. After each of 5 sample sets (consisting of two prints for each combination of layer heights per set), the build plate is again calibrated before the next 12 prints are realized (manual calibration with paper of $171 \mu\text{m}$ thickness). Detailed results for one print per parameter set are shown in Figure 3 and a comparison of all prints is shown in Figure 4.

As already discussed in Section 2.1, the height of the 1^{st} layer is significantly influenced by the calibration of the build plate, as shown in Figure 4a. For four of the five sample sets, the 1^{st} layer height of all prints differs significantly from the intended height of the model. Three of these sample sets show a lower height of the 1^{st} layer. Within each test sample set, the deviation of the 1^{st} layer height is of the same order of magnitude, independently of the model height of the first layer. These systematic errors are attributed to the build plate calibration. For the test sample set with a higher 1^{st} layer height (blue A shape triangle in Figure 4a), additionally extrusion errors are observed which lead to a high standard deviation.

Viewed across all prints, the average layer height of the 2^{nd} and 3^{rd} layers is higher than the nominal layer height (cf. Figure 4b). Sample standard deviations in the range of ± 8 to $\pm 18 \mu\text{m}$ are

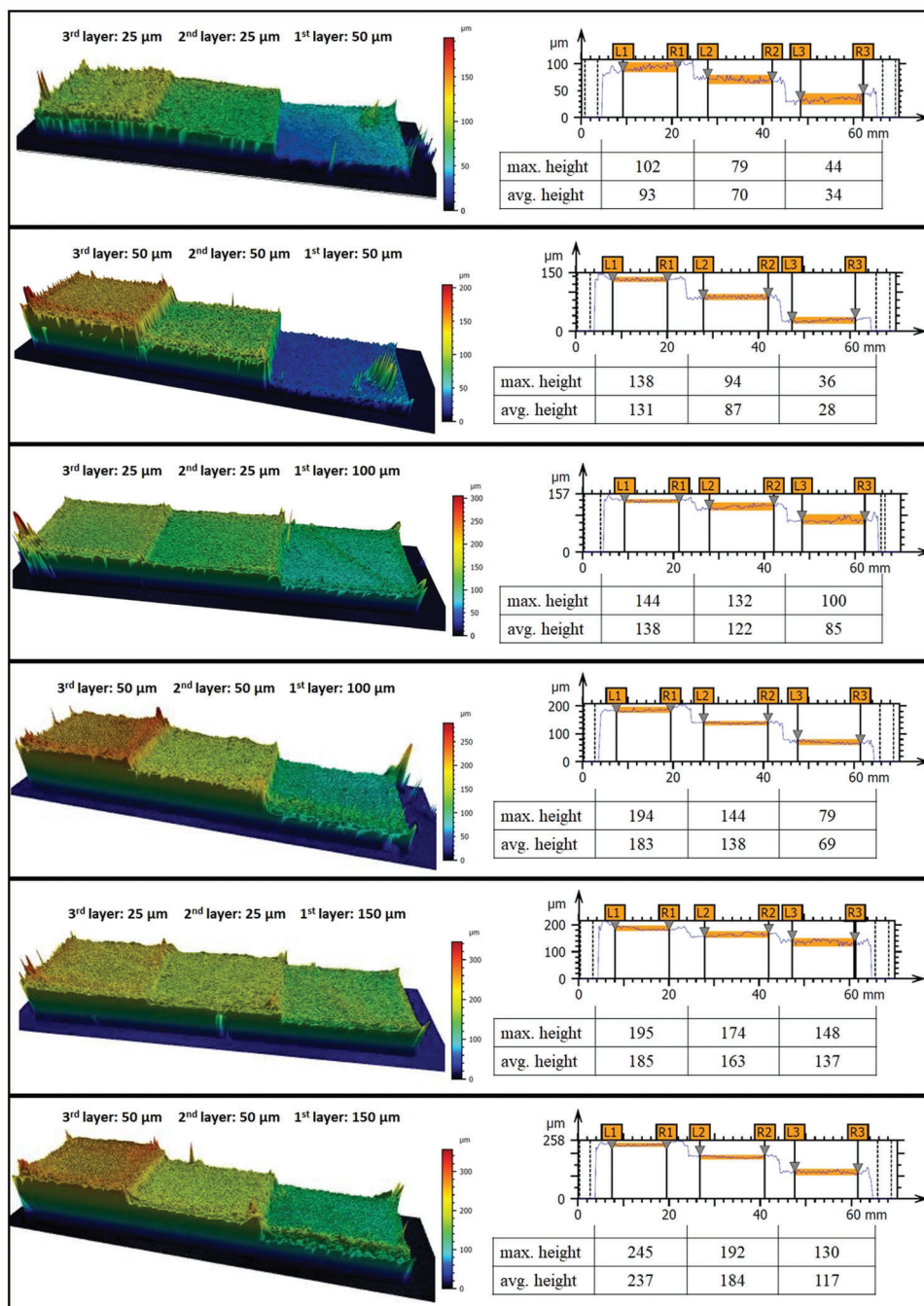


Figure 3. Chromatic-confocal distance measurements of the 3D printed small plates of PLA.

observed. It is hypothesized that the positioning mechanism of the build plate tends to overshoot. However, the Ultimaker 3 manufacturer indicates an accuracy of $\pm 2.5 \mu\text{m}$ for the z-position of its build plate. The extrusion rate is also assumed to affect the layer height, which might be affected itself by the filament feeder motor's limitations. However, a clear cause of this observation was not identified.

In case of the third layer, only 5 mm^3 or 10 mm^3 needs to be extruded in total (dimensions 10 mm by 20 mm with a nominal layer height of 0.025 or 0.050 mm). For a filament of 2.85 mm

diameter used here, this corresponds to a very short filament segment of 0.78 mm or 1.57 mm, respectively – and this short piece has to be melted and extruded evenly for printing one (third) layer.

For the 3D printing of small structures, a layer height of at least 100 μm for the 1st layer should be chosen. As discussed before, systematic deviations of the layer height in the range of $\pm 25 \mu\text{m}$ appear to be a result of the calibration routine. For a 50 μm high first layer, this would make up 50% of the nominal layer height and cannot be tolerated. For the upper layers,

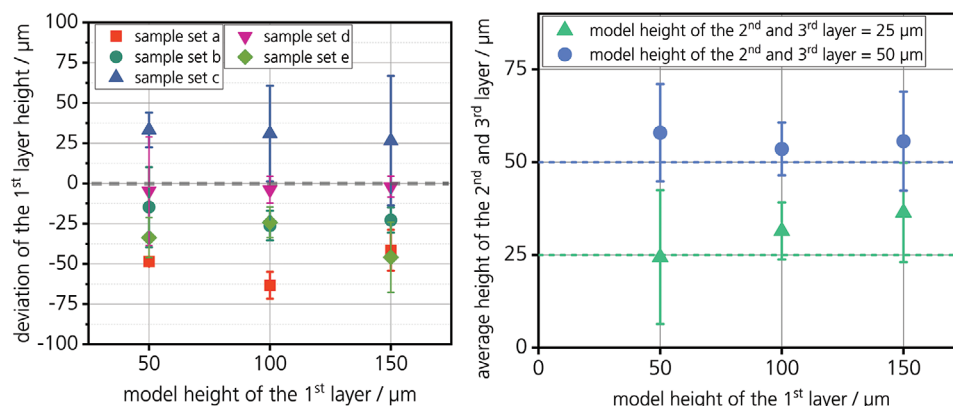


Figure 4. (Left) Deviation of the 1st layer height from the model height of the 1st layer for prints printed at 5 different times (two samples of each height are printed at the same time) with intermediate calibration. (Right) Average height (of all five print sets) of the 2nd and 3rd layers printed with 25 µm or 50 µm on top of a 1st layer with a model height of 50 µm, 100 µm, or 150 µm.

Table 1. Polymer compounds used for 3D printing.

#	Polymer	Additive	Additive amount / wt%
PLA	PLA	–	–
PVA	PVA	–	–
PLA/CNT-1	PLA	CNT	2
PLA/CNT-2	PLA	CNT	7
PVA/TiO ₂ -1	PVA	TiO ₂	5
PVA/TiO ₂ -2	PVA	TiO ₂	10

nominal layer heights of both 25 µm and 50 µm seem to be feasible, but in any case, the real layer heights have turned out to be several micrometers higher than anticipated.

2.3. 3D Printing of Polymer Compounds Containing Particulate Additives

In order to endow a polymer with useful properties like electrical conductivity or coloring, it is necessary to incorporate additives. In addition to the intended polymer compound properties, the behavior of the polymer compounds during 3D printing also changes. To study the influence of particulate additives, two different polymer compound systems are investigated, each of them with two different mass fractions of the additive. Their compositions are shown in Table 1. For the first system, PLA serves as the polymer matrix and carbon nanotubes are added to achieve electrical conductivity (PLA/CNT). The second compound consists of PVA and titanium oxide (PVA/TiO₂). PVA is water-soluble, thus the compound can be employed as a support structure. Furthermore, the titanium oxide additive creates a white coloring, which leads to a good visual contrast to the black PLA/CNT compounds.

To study the influence of three different nozzle diameters in combination with the different polymer compounds, PLA, PLA/CNT-2, PVA, and PVA–TiO₂-1 were extruded with constant material extrusion rate free hanging into the air and the widths of the solidified polymer extrudates (obtained 10 cm from the nozzle) were analyzed, see Figure 5.

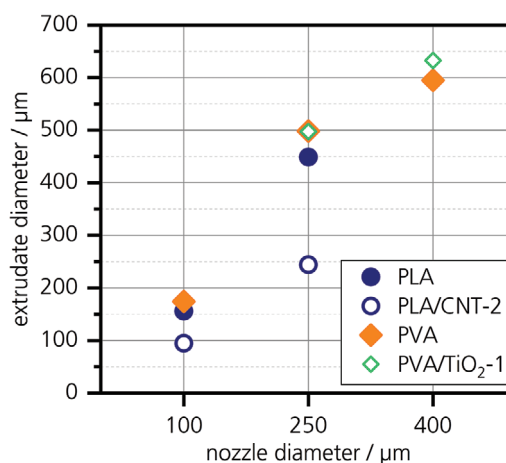


Figure 5. Influence of the nozzle diameter on the extrudate diameter of PLA, PLA/CNT-2, PVA, and PVA/TiO₂-1.

For both additive-free thermoplastic materials (PLA and PVA), a higher diameter of the extrudate in comparison to the nozzle size was detected for 100 µm and 250 µm nozzles. By contrast, PLA/CNT-2 containing 7 wt% CNT shows no such swelling in the extrusion. For PVA/TiO₂-1 containing 5 wt% TiO₂, an increased diameter of the extrudate is observed for a 250 µm AA-type nozzle accompanied by a fast blocking of the nozzle. Therefore, a 400 µm BB-type nozzle was additionally tested. An increased diameter of the extrudate is also observed with this nozzle.

Diameter expansion during extrusion depends largely on the interactions of the polymer molecules with each other or with any additive.^[16] Thus, the CNTs appear to significantly decrease the mobility of the polymer melt of the PLA/CNT compound here, so that in this case no expansion was observed after extrusion from the nozzle.

Besides the diameter swelling, a fast blocking of the nozzle is observed when the nozzle is too small. Therefore, at least a 250 µm AA-type nozzle is required for PLA/CNT and a 400 µm BB-type nozzle is required for PVA/TiO₂ to achieve continuous polymer extrusion.

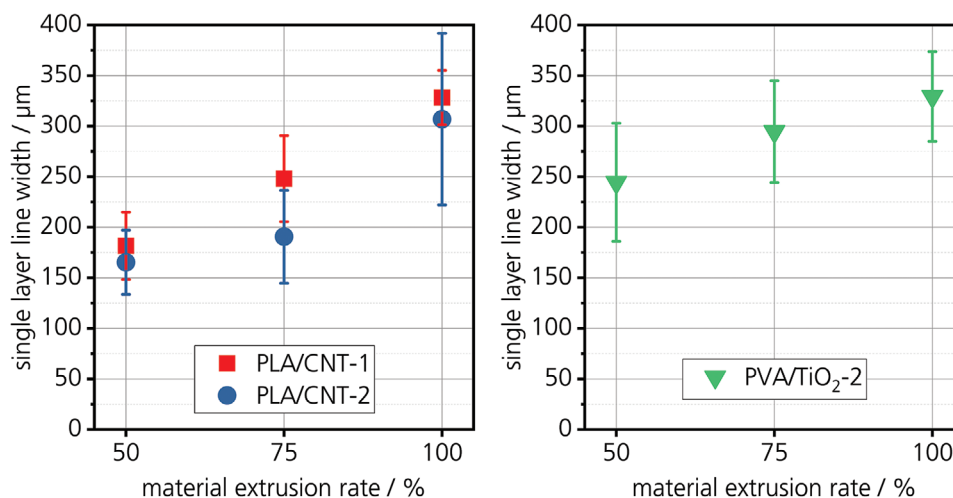


Figure 6. Printing results of single layer lines printed from PLA/CNT-1, PLA/CNT-2, and PVA/TiO₂-1 with a material extrusion rate of 100%, 75%, and 50%.

2.3.1. Minimum Line Width by 3D Printing of Single Layer Lines

Single layer lines are typically 1.2 to 1.5 times wider than the diameter of the used print nozzle.^[6] Therefore, for prints with a 400 μm nozzle, a single layer line width of 480–600 μm and for prints with a 250 μm nozzle, a single layer line width of 300–375 μm are expected. These line widths limit the 3D printing of small structures.

To reduce the single layer line width, the print settings were set to 80% nominal line width for all prints. This parameter is referenced to the nozzle diameter, which gives absolute values of 200 μm (250 μm nozzle, PLA/CNT) and 320 μm (400 μm nozzle, PVA/TiO₂), respectively. The nominal line width is a virtual parameter in the printing preparation; along with the nominal layer height, it determines the amount of material required to form the desired structure. At a given nozzle velocity, this parameter is practically reflected in the absolute material extrusion rate. The latter can moreover be adjusted by a constant factor. In the present study, this adjustment factor of the extrusion rate was varied between 100% and 50% to investigate the influence of the extrusion rate on the single layer line width.

The print results of single layer prints with a line height of 100 μm at 210 °C are shown in **Figure 6**, whereas **Figure 7** illustrates the s-shape line print pattern and gives an overview of the typical appearances of the prints under these conditions.

For all three materials, a decrease of the single layer line width is observed with the reduction of the material extrusion rate. PLA/CNT-1 containing 2 wt% of CNT shows average line widths of 328 μm, 248 μm, and 182 μm for 100%, 75%, and 50% extrusion rates, respectively. The print quality also decreases, as shown in **Figure 7**. However, even with a material extrusion rate of 50%, continuous single layer lines are obtained with one exception. PLA/CNT-2 containing 7 wt% of CNT shows different results. The average line width decreases from 307 μm to 191 μm to 165 μm. Already at a material extrusion rate of 100%, a large variation of line width is observed and with 75% continuous single layer lines are not obtained for all prints. PVA/TiO₂-2 containing 10 wt% TiO₂ shows a decrease of the average line width from

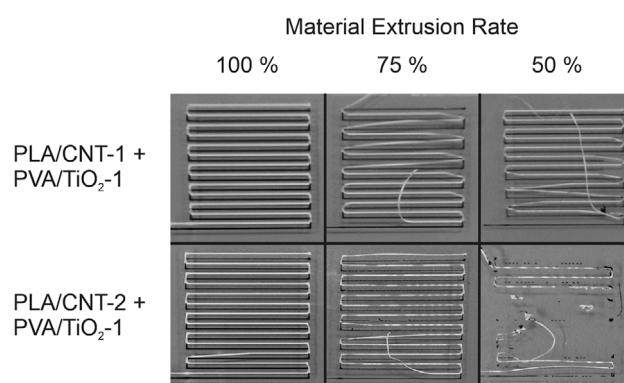


Figure 7. Single layer line width of PLA/CNT-1, PLA/CNT-2 (250 μm nozzle), and PVA/TiO₂-2 (400 μm nozzle) printed at 210 °C with a material extrusion rate of 100%, 75%, and 50% and a single layer line width of 80% in the print model.

329 μm to 295 μm to 244 μm. For this material, not all printed lines adhere well to the build plate. This behavior is already observed in some cases at a material extrusion rate of 100%, at 75%, the print quality deteriorates significantly and at 50%, adhesion of the print is only rarely observed.

From these observations, it can be determined that for the 3D printing of small structures from PLA/CNT and PVA/TiO₂, a line width of approximately 300 μm is quite possible for both a) a main structure (PLA/CNT) printed with a 250 μm AA nozzle and b) a supporting structure (PVA/TiO₂) printed with a 400 μm BB nozzle. Furthermore, the line width of the PLA/CNT main structure can be reduced even more to the range of about 200 μm. However, the print quality decreases with increasing CNT amount.

2.3.2. 3D Printing of Small Porous Structures

Based on the abovementioned results for the layer thickness and the achievable line width, small porous structures were designed and printed. The main structure consists of parallel lines of the

material PLA/CNT-2 (nominal line width 200 μm). Between two lines, a channel-like empty space is designed, which is filled with the material PVA/TiO₂-2 (nominal line width 320 μm) during the printing process; afterward, the supporting material is dissolved with water. As already mentioned, the printed structures are actually wider than the nominal line width, therefore the lines of the main and supporting structures were printed at a distance of 375 μm (with reference to the respective center of the printed line). The porous structure in the here investigated case consists of three layers with a nominal layer thickness of 100 μm for the first layer and 25 μm for the second and third layers. The orientation of the printed lines differs by 90° from the first to the second layer, resulting in a grid-like structure. The lines of the third layer arrange parallel to the first but offset by 320 μm . As mentioned before, the black material PLA/CNT-2 contains 7 wt% CNTs and is extruded through a nozzle with 250 μm diameter (type of inner shape: AA). The white material PVA/TiO₂-2 used for manufacturing the small porous structures contains 10 wt% TiO₂ and is printed with a nozzle of 400 μm in diameter (type of inner shape: BB). In both cases, the nozzle temperature was set to 210 °C. With these parameters, small porous structures can be successfully produced with an Ultimaker 3. However, the structure is mechanically fragile. The design of component should take this into account.

Figure 8 shows the successful printing of such a lattice-like structure of PLA/CNT-2 (black) before the extraction of the supporting material PVA/TiO₂-2 (white). In **Figure 8a**, only the bottom layer is shown (100 μm nominal layer height), here the two materials are in contact. A top view onto the upper (third) layer is shown in **Figure 8b**, with the middle layer is partially exposed. Here, the two different materials do not touch each other within the layer. If necessary, this can be corrected by adjusting the design of the lattice-like structure.

To obtain more mechanically stable structures with complete closed layers, the printing parameters were adjusted. All layers were printed with 100 μm height using a 400 μm nozzle for both materials to widen the printed line width. Additionally, the line distance was adjusted to 700 μm for the 1st layer, 650 μm for the 2nd layer, and 575 μm for 3rd layer. **Figure 9** shows the small porous structure of this adaptation: **Figure 9a** shows the complete printed structure. **Figure 9b** shows a microscope image of the 3rd layer – the contact between PLA/CNT and PVA/TiO₂ is given without gaps. **Figure 9c** shows an image of the final small porous structure after the removal of the PVA/TiO₂ component. The investigation of their conductivity and mechanical stability is part of future investigations.

3. Conclusion

Based on analyses of the influence of the calibration of the building plate, the heights of the 1st, 2nd, and 3rd layers, the effect of particulate additives on the printing behavior of polymer compound, and the width of a single printed line using PLA, PLA/CNT, and PVA/TiO₂, printing parameters for the production of grid-shaped scaffold structures by FFF with an Ultimaker 3 were investigated.

Small porous structures of PLA/CNT with a line width of 200 μm can be produced by printing PLA/CNT in combination with the soluble support material PVA/TiO₂. For small porous

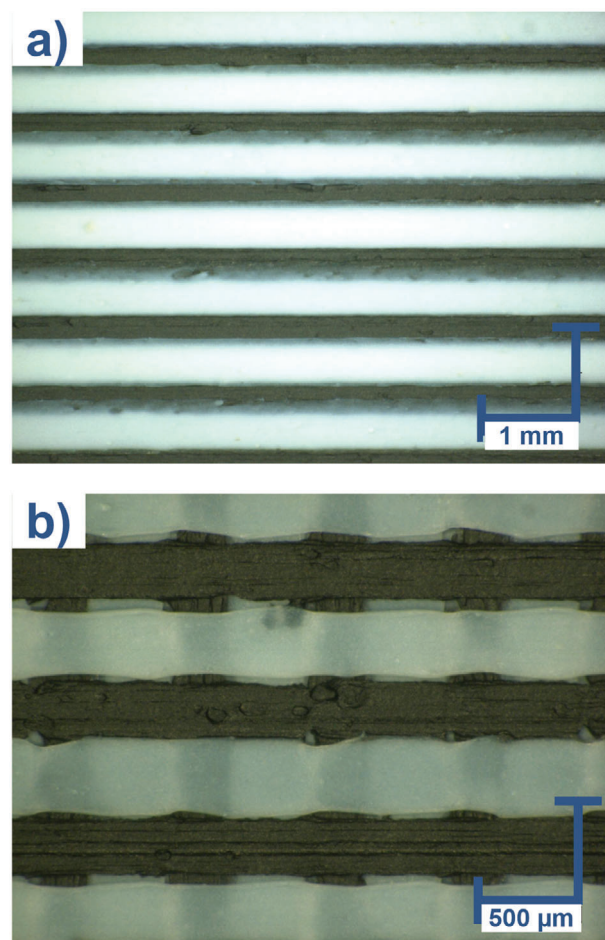


Figure 8. Small porous structures printed from PLA/CNT-2 (black) and PVA/TiO₂-2 (white); a) view on the first printed layer, b) view on the third layer with parts of the second layer exposed; PLA/CNT: 250 μm nozzle @210 °C, PVA/TiO₂: 400 μm nozzle @210 °C.

structures with a good component quality, a layer height of 100 μm for each layer should be chosen.

4. Experimental Section

Materials: The commercially available filaments PLA natural from Inofil3D (melting point: 145–160 °C; density: 1.26 g cm⁻³), PVA natural from Ultimaker (melting point: 163 °C; density: 1.23 g cm⁻³), and PLA/CNT filament f-electric from Functionalize, Inc. (7 wt% CNT) were used. For the production of polymer compounds, PLA Purapol L130 from Corbion (melting point: 175 °C; density: 1.24 g cm⁻³), PVA Mowiol 3D 2000 from Kuraray (melting point: 180–190 °C; density: 0.6–0.9 g cm⁻³), CNT NC7000 from Nanocyl (length: 1.5 μm ; diameter: 9.5 nm), and Aeroxide TiO₂ P25 (average primary particle size: 21 nm) from Evonik were used. All filaments from PVA were stored under argon and dried frequently at 60 °C for 20 h under vacuum.

Compounding and Filament Production: Commercial filaments and in-house produced filaments were used for the AM. To produce filaments, polymer compounds were prepared by melt extrusion of grounded polymeric material premixed with powdery polymer additives using a twin-screw 16 mm HAAKE-Polylab/Rheocord by ThermoFisher Scientific and a small-scale filament extruder 3devo Next 1.0 advanced from 3devo

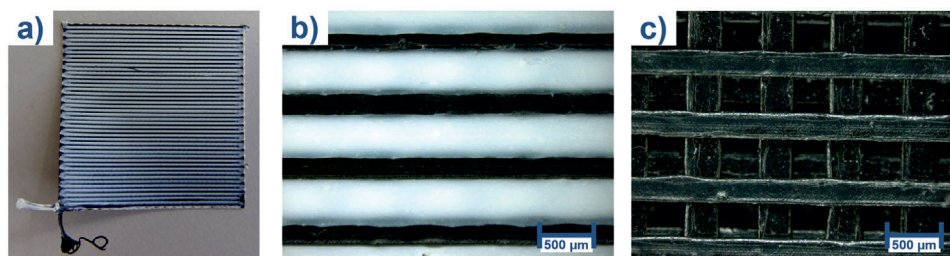


Figure 9. Small porous structure printed from PLA/CNT-1 (black) and PVA/TiO₂-2 (white); PLA/CNT: 400 µm nozzle @210 °C, PVA/TiO₂: 400 µm nozzle @210 °C; a,b) small porous structure before water treatment, c) small porous structure after water treatment.

B.V., Netherlands. The compositions of the used polymer compounds are shown in Table 1.

FFF Printing: The used FFF 3D printer was a desktop twin-nozzle FFF printer Ultimaker 3 from Ultimaker B.V., Netherlands. The position accuracy of the Ultimaker 3 was specified as 12.5 µm in the x- and y-directions and 2.5 µm in the z-direction.^[8] For this study, different nozzles from Ultimaker B.V. (type-AA nozzles with a nozzle diameter of 250 µm and type-BB nozzles with a nozzle diameter of 400 µm) or from 3D Solex, Norway (type-AA nozzle with a nozzle diameter of 100 µm) and the glass building plate from the Ultimaker 3 as well as float glass building plates with a thickness variation of 15 µm were used.

The step-like test samples used in this work were modeled using FreeCAD (version 0.18) followed by a slicing step using Cura (version 4.2). However, this method was not suitable for reproducibly printing of single lines and single-line-based porous network structures. Therefore, all digital models that contained single line segments (like samples discussed in Sections 2.3.1 and 2.3.2) were programmed manually in G-code (language: Griffin) using RepetierHost (version: 2.1.6) software for visualization.

Characterization—Calibration of the Distance between Building Plate and Printing Nozzle: A step-like sample with a base area of 20 × 60 mm² and a total thickness of 170 µm of the first step, 220 µm of the second step, and 270 µm of the third step was designed using FreeCAD and Cura for slicing. The distance between building plate and printing nozzle was calibrated by using a A4 printing paper with 100 g m⁻² (thickness: 113 ± 5 µm, measured with a micrometer screw from Mitutoyo), a A4 printing paper with 160 g m⁻² (thickness: 171 ± 5 µm, measured with a micrometer screw from Mitutoyo), a feeler gauge (nominal thickness: 150 µm), and the autocalibration program of the Ultimaker 3. Each calibration procedure was tested twice. In each test, two step-like samples were printed side by side using a type-AA nozzle with 250 µm diameter at 215 °C with PLA natural from Innofil3D. The thickness of each sample was measured at four locations of each step with a micrometer (accuracy: 1 µm).

Characterization—3D Printing of Small Plates: For the study of 3D small plates, step-like samples with a base area of 15 × 60 mm² were printed. The thickness of the first layer was 50 µm, 100 µm, or 150 µm. For each of these first layer thicknesses, a thickness of 25 µm or 50 µm for the second and third layers were studied. 5 times, 12 samples were printed side by side, two for each first layer–second/third layer combination. Before the print of each test sample set, the building plate was calibrated using the A4 printing paper with 160 g m⁻² (thickness: 171 ± 5 µm). The prints were performed with a type-AA nozzle with 250 µm diameter at 200 °C with PLA natural from Innofil3D. The chromatic-confocal distance measurements of the samples were performed with a 3D confocal microscope µscan from NanoFocus AG without removing the printed samples from the building plate.

Characterization—3D Printing Behavior of Polymer Compounds: To determine the 3D printing behavior of polymer compounds, the polymer compounds were extruded with constant material extrusion rate into the air and the width of the obtained polymer extrudates were measured on at least three positions using a Keyence VHX-100 with a magnification of 100×–1000×. Each polymer compound was analyzed 3 times.

Characterization—3D Printing of Single Layer Lines: Single layer lines were printed at 210 °C with PLA/CNT-1 or PLA/CNT-2 with a 250 µm AA nozzle and PVA/TiO₂-2 with a 400 µm BB nozzle. The layer height was 100 µm and the single layer line width was 80% of the nozzle diameter. The material extrusion rate was 100%, 75%, or 50%. An “S”-like structure with 13 lines with a length of 25 mm and a distance between the lines of 2 mm were printed with PLA/CNT. The same structure was printed with PVA/TiO₂ into the space between the lines of the PLA/CNT structure. For each material extrusion rate, three structures were printed on one building plate. The print was repeated once. The single layer line width was measured using a Keyence VHX-100 optical microscope with a magnification of 100×–1000×.

Characterization—3D Printing of Small Porous Structures: Small porous structures were printed at 210 °C with PLA/CNT-1 using a 250 µm or a 400 µm AA nozzle and PVA/TiO₂-2 using a 400 µm BB nozzle. For the first approach, layer heights of 100 µm for the 1st layer and 25 µm for the 2nd and 3rd layers were used. In the final optimized structure, all three layers were printed with a height of 100 µm. Similar to Subsection “Characterization—3D Printing of Single Layer Lines,” “S”-like structures were printed. PVA/TiO₂ was printed into the space between the lines of the PLA/CNT compound. The 2nd layer was rotated by 90° compared to the 1st and 3rd layers. The structures were analyzed using the optical microscope Keyence VHX-100 with a magnification of 100×–1000×.

Acknowledgements

Financial support by Vector Stiftung in the context of the project 3D-PakT, project number P2018-0177, is greatly acknowledged. Experimental support by Matthias Stricker, Patrick Weiss, and Hubert Weyrauch, all from Fraunhofer Institute for Chemical Technology ICT, is also acknowledged.

Open access funding enabled and organized by Projekt DEAL.

Conflict of Interest

The authors declare no conflict of interest.

Data Availability Statement

The data that support the findings of this study are available from the corresponding author upon reasonable request.

Keywords

3D printing, additive manufacturing, fused filament fabrication, polymer compounds, small scaffold structures

Received: February 10, 2022

Revised: July 12, 2022

Published online:

- [1] a) M. H. Too, K. F. Leong, C. K. Chua, Z. H. Du, S. F. Yang, C. M. Cheah, S. L. Ho, *Int. J. Adv. Des. Manuf. Technol.* **2002**, 19, 217; b) K. Chin Ang, K. Fai Leong, C. Kai Chua, M. Chandrasekaran, *Rapid Prototyping J.* **2006**, 12, 100; c) H.-J. Yen, C.-S. Tseng, S.-H. Hsu, C.-L. Tsai, *Biomed. Microdevices* **2009**, 11, 615; d) D. Espalin, K. Arcaute, D. Rodriguez, F. Medina, M. Posner, R. Wicker, *Rapid Prototyping J.* **2010**, 16, 164; e) D. W. Huttmacher, T. Schantz, I. Zein, K. W. Ng, S. H. Teoh, K. C. Tan, *J. Biomed. Mater. Res.* **2001**, 55, 203.
- [2] J. Korpela, A. Kokkari, H. Korhonen, M. Malin, T. Närhi, J. Seppälä, *J. Biomed. Mater. Res., Part B* **2013**, 101B, 610.
- [3] a) D. W. Huttmacher, *Biomaterials* **2000**, 21, 2529; b) J. Kim, S. McBride, B. Tellis, P. Alvarez-Urena, Y.-H. Song, D. D. Dean, V. L. Sylvia, H. Elgendy, J. Ong, J. O. Hollinger, *Biofabrication* **2012**, 4, 25003.
- [4] S. J. Kalita, S. Bose, H. L. Hosick, A. Bandyopadhyay, *Mater. Sci. Eng., C* **2003**, 23, 611.
- [5] Q. Chen, J. D. Mangadlao, J. Wallat, A. de Leon, J. K. Pokorski, R. C. Advincula, *ACS Appl. Mater. Interfaces* **2017**, 9, 4015.
- [6] B. N. Turner, S. A. Gold, *Rapid Prototyping J.* **2015**, 21, 250.
- [7] B. N. Turner, R. Strong, S. A. Gold, *Rapid Prototyping J.* **2014**, 20, 192.
- [8] *Ultimaker 3: Installations- und Benutzerhandbuch*, Ultimaker B.V., Utrecht **2017**.
- [9] D. Brackett, I. Ashcroft, R. Hague, *Solid Freeform Fabr. Symp. Proc.* **2011**, 1, 348.
- [10] X. Wang, M. Jiang, Z. Zhou, J. Gou, D. Hui, *Composites, Part B* **2017**, 110, 442.
- [11] R. W. Gray, D. G. Baird, J. Helge Böhn, *Rapid Prototyping J.* **1998**, 4, 14.
- [12] S. Masood, W. Song, *Mater. Des.* **2004**, 25, 587.
- [13] A. Dorigato, V. Moretti, S. Dul, S. H. Unterberger, A. Pegoretti, *Synth. Met.* **2017**, 226, 7.
- [14] N. Sandler, I. Salmela, A. Fallarero, A. Rosling, M. Khajeheian, R. Kolakovic, N. Genina, J. Nyman, P. Vuorela, *Int. J. Pharm.* **2014**, 459, 62.
- [15] D. Chalissery, T. Pretsch, S. Staub, H. Andrä, *Polymers* **2019**, 11, 1005.
- [16] J. Goff, T. Whelan, *The Dynisco Extrusion Processors Handbook*, 2nd ed., Dynisco, Franklin, MA **2000**.